

Article

Enhanced Bioconversion of Methane to Biodiesel by *Methylosarcina* sp. LC-4

Nivedita Sana ¹, Dali Naidu Arnepalli ^{1,*} and Chandraraj Krishnan ²¹ Department of Civil Engineering, Indian Institute of Technology Madras, Chennai 600036, India² Department of Biotechnology, Indian Institute of Technology Madras, Chennai 600036, India

* Correspondence: arnepalli@iitm.ac.in

Abstract: The conversion of methane into liquid biofuels using methane-consuming bacteria, known as methanotrophs, contributes to sustainable development, as it mitigates the problem of climate change caused by greenhouse gases and aids in producing cleaner and renewable energy. In the present research, an efficient methanotroph, *Methylosarcina* sp. LC-4, was studied as a prospective organism for biodiesel production using methane. The methane uptake rate by the organism was enhanced 1.6 times and 2.35 times by supplementing LC-4 with micronutrients, such as copper and tungstate, respectively. This unique ability of the isolated organism enables the deployment of methanotrophs-based processes in various industrial applications. A Plackett–Burman statistical (PBD) design was used to quantify the role of the micronutrients and other media components present in the nitrate minimal salt media (NMS) in biomass and fatty acid methyl esters (FAME) yields. Nitrate, phosphate, and tungstate had a positive effect, whereas copper, magnesium, and salinity had a negative effect. The modified NMS media, formulated according to the results from the PBD analysis, increased the FAME yield (mg/L) by 85.7%, with the FAME content of $13 \pm 1\%$ (*w/w*) among the highest reported in methanotrophs. The obtained FAME consisted majorly (~90%) of C₁₄–C₁₈ saturated and monounsaturated fatty acids, making it suitable for use as biodiesel.

Keywords: biodiesel; biological gas to liquid; methanotroph

Citation: Sana, N.; Arnepalli, D.N.; Krishnan, C. Enhanced Bioconversion of Methane to Biodiesel by *Methylosarcina* sp. LC-4. *Sustainability* **2023**, *15*, 505. <https://doi.org/10.3390/su15010505>

Academic Editor: Shashi Kant Bhatia

Received: 15 November 2022
Revised: 15 December 2022
Accepted: 22 December 2022
Published: 28 December 2022



Copyright: © 2022 by the authors. Licensee MDPI, Basel, Switzerland. This article is an open access article distributed under the terms and conditions of the Creative Commons Attribution (CC BY) license (<https://creativecommons.org/licenses/by/4.0/>).

1. Introduction

Renewable fuels have gained tremendous importance due to the ever-increasing demand for energy and depleting reserves of traditional fossil fuels. The biological production of liquid fuels using plants or microbes is a promising alternative to the existing petroleum-based fuels [1]. Microbially produced biofuel is often advantageous over other sources of biofuels because of their short generation time, faster growth rates, and ease of upscaling. Moreover, microbial processes are less affected by geographical and environmental factors and are often less labor-intensive [2,3]. Over the past few years, microbes such as yeasts, microalgae, and several bacteria have been exploited for biodiesel production because they assimilate lipids with more than 20% of their cell dry weight [4]. However, the economic feasibility of these microbes for biofuels is determined mainly by the carbon feedstock used, which accounts for 50–70% of the total manufacturing cost [5]. Thus, the carbon source for biomass production is the most critical factor influencing biofuel commercialization and industrial production.

In recent years, the usage of methane as a next-generation carbon feedstock in biotechnological processes has attracted the attention of researchers [6]. Methane is also a renewable feedstock and the lowest-cost feedstock-generated by-product of the biological degradation of organic matter [7,8]. It is a potent greenhouse gas (GHG), and its levels in the atmosphere are increasing at an alarming rate, mainly due to anthropogenic sources, contributing to 30% of global warming today [9]. High-concentration sources of methane, such as natural and shale gas, can be tapped and used for beneficial purposes [10]. However, low

methane concentrations from landfills, wastewater treatment plants, and coal mines have little commercial value and are generally flared or left in the environment, contributing to global warming [11]. Recently, biological gas-to-liquid (Bio-GTL) technology has emerged as a solution to utilize these low-concentration methane sources [5,12,13], thus, reducing the production cost and being a feasible solution to global warming by GHGs.

Bio-GTL technology of methane to next-generation fuels exploits methanotrophic bacteria that can naturally oxidize and assimilate methane at atmospheric temperature and pressure [10,14]. Methanotrophs have enormous industrial potential to transform methane generated from waste into value-added products, such as methanol, single-cell protein, bioplastics, and biodiesel [15–17]. However, most of these processes are laboratory studies and function as a testbed for methane-based biorefineries.

Methanotrophs are a diverse group of organisms that have not been entirely explored due to the difficulty in isolating them in pure cultures, and congruently deciding upon an optimal species for biodiesel production is impossible with the limited knowledge available [17,18]. Although there have been prior reports on biodiesel production using methanotrophs, the research is still in its infancy, restricted to a few laboratory strains, such as *Methylomicrobium buryatense* and *Methylocystis* sp. [19,20]. Moreover, most studies on methanotrophic bacteria have been carried out in nitrate minimal salt (NMS) media, whereas optimization of both macro and micronutrients in the media is often necessary for improved yields of biomass and derived value-added products at an industrial scale [17]. Compared to other bacteria, methanotrophs have unique nutritional requirements, including such micronutrients as copper, lanthanides (like cerium), and tungsten, which are cofactors for key enzymes of the central methane oxidation pathway. The productivity of methanotrophs depends on the methane monooxygenase (MMO) expressed to oxidize methane to methanol and the central metabolic pathway governing the overall carbon capture efficiency [10].

From the literature, particulate membrane-associated methane monooxygenase (pMMO)-expressing type-I methanotrophs that use the ribulose monophosphate pathway (RuMP) exhibited the highest growth rate, methane-oxidizing, and assimilation capability compared to other methanotrophs [18,21]. Our previous study reported a robust, fast-growing pMMO-expressing type-I methanotroph *Methylosarcina* LC-4 with a high specific methane uptake rate. The isolate LC-4 has a high carbon conversion efficiency, assimilating ~70% of methane supplied, and requires lower oxygen per methane oxidized compared to other known methanotrophs (lesser cost of aeration) [22]. Furthermore, LC-4, an obligate pMMO-expressing methanotroph, is expected to produce extensive intracytoplasmic membranes (ICM) to host this membrane-associated protein [23]. These membrane lipids are phospholipids containing C₁₄–C₁₈ saturated and monounsaturated fatty acids and are suitable for use in biodiesel [22,24]. The present study explores biodiesel as a by-product of methane mitigation by *Methylosarcina* sp. LC4 and implores the role of micronutrients (copper, cerium, tungstate) and macronutrients (such as nitrogen, phosphorus, and magnesium) in this process.

2. Materials and Methods

2.1. Culture and Growth Conditions

Methylosarcina sp. LC-4 isolated from the leachate sample of the municipal solid waste dumpsite, Chennai, India, was used for the present study. The organism was grown on Nitrate minimal salt (NMS) media containing 0.26 g/L KH₂PO₄, 0.62 g/L Na₂HPO₄·7H₂O, 1 g/L KNO₃, 1 g/L MgSO₄·7H₂O, 0.2 g/L CaCl₂·H₂O, 3.8 mg/L Fe-EDTA, and 0.5 mg/L Na₂Mo·4H₂O supplemented with 1 mL/L trace element solution and 10 mL/L vitamin solution. The trace element solution contained 500 mg/L FeSO₄·7H₂O, 400 mg/L ZnSO₄·7H₂O, 20 mg/L MnCl₂·7H₂O, 50 mg/L CoCl₂·6H₂O, 10 mg/L NiCl₂·6H₂O, 15 mg/L H₃BO₃, and 318 mg/L EDTA-Na₂. The vitamin solution contained 2 mg/L biotin, 2 mg/L folic acid, 5 mg/L thiamine HCl, 5 mg/L calcium pantothenate, 2 mg/L vitamin B12, 5 mg/L riboflavin, 25 mg/L nicotinamide, 2 mg/L lipoic acid, 2 mg/L pyridoxal, and 2 mg/L

4-aminobenzoic acid. The organism was grown in a 150 mL Erlenmeyer flask with 30 mL NMS media and sealed with a silicone sleeve stopper septa. Methane (12% *v/v*) was injected into this flask by a 10 mL gas-tight Hamilton syringe and incubated at 30 °C, 200 rpm.

2.2. Assessing the Effect of Trace Metal Ions on Methane Oxidation

Organism grown on 12% (*v/v*) of methane was used as the preculture for the experiments, and 2 mL of this preculture was inoculated in 28 mL of NMS media. NMS media was supplemented with varying concentrations of copper (0–150 µM), cerium (0–10 µM), or tungstate (0–1 µM), as specified in the experiment. Wherever the concentration of copper is not specified, NMS media supplemented with 10 µM of copper was used. The initial methane concentration of 6% *v/v* was maintained. The concentrations of methane, oxygen, and carbon dioxide were monitored every 3 h interval for 30 h. The initial and final biomass concentrations were assessed using the optical density measurement at 600 nm. All the experiments were done in triplicates. The Boltzmann equation (Equation (1)) was used to determine the methane oxidation or uptake rate [22].

$$y = \frac{dX}{dt} = \frac{A_1 - A_2}{1 + e^{(x-x_0)/dx}} + A_2 \quad (1)$$

where y and X represent the gas concentration (methane/oxygen/carbon dioxide) and time, respectively, and A_1 , A_2 , d , and x_0 are the Boltzmann parameters.

The biomass yield coefficient was determined by using Equation (2).

$$Y_{X/S} = \frac{\text{gram of dry biomass weight}}{\text{gram of substrate consumed}} \quad (2)$$

where $Y_{X/S}$ is the biomass yield coefficient

2.3. Scanning Electron Microscopy with Energy Dispersive X-ray Analysis (SEM-EDX)

The organism grown in the NMS media was concentrated by centrifuging at 10,000 rpm for 10 min. The obtained culture was washed with 1% (*w/v*) NaCl solution and centrifuged. The culture was lyophilized and sputter-coated with gold for observation under a scanning electron microscope with an EDX facility (SEM-EDX).

2.4. Transesterification and Extraction of Fatty Acid Methyl Esters from Biomass

Fatty acid methyl esters (FAME) were prepared by direct transesterification of biomass in a single step by avoiding the step of lipid extraction [25]. Methanol: H₂SO₄ (2:1 *v/v*) solution of 10 mL was added to 10 mg of dry biomass, along with 100 µL of heptadecanoic acid (C17:0, 1 mg/mL) to act as an internal standard, and stirred at 150 rpm at 70 °C under reflux for 6 h. FAME formed were then extracted by adding 20 mL of non-polar solvent hexane. The mixture was allowed to stand for 10 min for phase separation, and the hexane layer was separated. A rotary evaporator was used to concentrate the obtained organic phase at 50 °C. The concentrated FAME was made up to 1 mL by adding hexane, and the filtrate was analyzed using gas chromatography.

2.5. Optimization of Media Components by Plackett–Burman Design Method

A Plackett–Burman design (PBD) is a statistical method to screen important factors in an experiment. The PBD experiment to identify and study the influence of essential nutrients on lipid (FAME) production in *Methylosarcina* sp. LC-4 was generated using Design-Expert software version 11 (Stat-Ease Inc., Minneapolis, MN, USA). For this study, seven media components were chosen (A to G in Table 1). Each component was set at a high concentration (+1) and low concentration (−1), as depicted in Table 1. The experiments were carried out in 2.5 L glass bottles with a 600 mL working volume. NMS media were modified per the PBD experiments' specifications (Table 2). A 30 mL preculture was added and sealed

with a Teflon stopper, silicone septa, and a screw cap. Initial methane concentration of 18% *v/v* was maintained and incubated at 30 °C at 450 rpm for 30 h. All experiments were done in triplicates (in 3 groups), and biomass (mg/L) and FAME yield (mg/L) was determined. The FAME yield was considered the output variable for the PBD model. PBD follows a linear method to quantify the contribution of each component on FAME and neglects the interaction between them. From the ANOVA analysis, components of the NMS media that showed a *p*-value < 0.05 were considered significant in the model. PBD following the first-order polynomial equation was used to describe the model (Equation (3)).

$$Y = \beta_0 + \sum \beta_i X_i \quad (3)$$

where *Y* represents the average FAME yield (mg/L), β_0 is the model's intercept, β_i is the linear coefficient, and X_i is the value of the individual factor.

Table 1. The coded and actual values of NMS media components used in the Plackett–Burman design.

Component	Unit	Designation	Coded Values	
			−1	+1
Nitrogen (KNO ₃)	mM	A	1	10
Phosphorus (KH ₂ PO ₄ -Na ₂ HPO ₄ buffer)	mM	B	0.42	4.20
Copper (CuSO ₄)	μM	C	10	75
Tungstate (Na ₂ WO ₄)	μM	D	0	0.5
Cerium (CeCl ₃)	μM	E	0	10
Magnesium (MgSO ₄)	mM	F	0.81	8.10
Salinity (NaCl)	mM	G	0	171

Table 2. Plackett–Burman design and the observed production of biomass and FAME yield.

Run	A	B	C	D	E	F	G	Biomass (mg/L)	FAME Yield (mg/L)
1.	+1	−1	−1	−1	+1	+1	+1	56 ± 1.3	6.3 ± 0.1
2.	+1	+1	−1	−1	−1	+1	+1	53 ± 3.4	5.4 ± 0.4
3.	+1	+1	+1	−1	−1	−1	+1	38.8 ± 3	4.1 ± 0.3
4.	+1	+1	+1	+1	−1	−1	−1	302.2 ± 9.5	48.7 ± 1.6
5.	−1	+1	+1	+1	+1	−1	−1	293.3 ± 1	30.7 ± 3.5
6.	−1	−1	+1	+1	+1	+1	−1	42 ± 2	4.6 ± 0.2
7.	−1	−1	−1	+1	+1	+1	+1	57.6 ± 2.5	5.9 ± 0.3
8.	−1	−1	−1	−1	−1	−1	−1	312.7 ± 11.6	32.7 ± 1.2

2.6. Analytical Techniques

2.6.1. Ultraviolet (UV)-Visible Spectrophotometer

The biomass concentration was determined based on the optical density at 600 nm (OD₆₀₀), obtained using a UV-visible spectrophotometer (Agilent Cary 100, Agilent). The following correlation was used to determine the dry biomass concentration (Equation (4)). This correlation has been obtained in our previous study by plotting dry biomass weight versus OD₆₀₀ of the LC-4 culture [22].

$$\text{Dry biomass concentration} \left(\frac{\text{mg}}{\text{L}} \right) = \frac{OD_{600}}{0.00143} \quad (4)$$

2.6.2. Gas Chromatography (GC)

Agilent GC 7890A, equipped with a thermal conductivity detector (TCD) and flame ionization detector (FID), was used for the gas and FAME analysis, respectively.

Gas analysis

GC analyzed the headspace gas with a TCD detector. Approximately 0.5 mL of headspace gas sample was collected in a 5 mL Hamilton gas-tight syringe, injected in GC with carboxen 1000 packed column as the stationary phase, and analyzed as per the previously reported method [22].

FAME analysis

The FAME was analyzed by GC equipped with an HP-5 column (30 m, internal diameter 0.25 mm, film thickness 0.25 μm) with an FID detector. Helium was used as the carrier gas. Injector and detector temperatures were set at 280 $^{\circ}\text{C}$. The oven temperature was programmed as follows: 120 $^{\circ}\text{C}$ hold for 5 min, 2 $^{\circ}\text{C}/\text{min}$ to 175 $^{\circ}\text{C}$, hold for 15 min, 10 $^{\circ}\text{C}/\text{min}$ to 220 $^{\circ}\text{C}$, hold for 10 min, 10 $^{\circ}\text{C}/\text{min}$ to 280 $^{\circ}\text{C}$, and hold for 15 min. Then, 1 μL of filtered FAME sample was injected into the injector port at a split ratio of 10:1. The chromatography data were acquired, and the total FAME content was calculated by using the European standard method EN14103:2011 by expressing in terms of mass fraction of methyl C17:0 internal standard (Equation (5)) [26].

$$\text{Total FAME (mg)} = \frac{\Sigma A - A_{IS}}{A_{IS}} \times C_{IS} \times V_{IS} \quad (5)$$

where ΣA is the total peak area (C12:0–C22:0), A_{IS} is the peak area of internal standard heptadecanoic acid methyl ester (C17:0), C_{IS} is the concentration of internal standard, and V_{IS} is the volume of the internal standard taken for the transesterification reaction.

The % FAME was calculated as a percent of the weight of the dry biomass sample initially taken for the transesterification process (Equation (6)).

$$\% \text{ FAME} = \frac{\text{Total FAME}}{\text{Biomass weight (mg)}} \times 100 \quad (6)$$

The FAME yield (mg/L) at different growth conditions was estimated by the following Equation (7), where the dry biomass concentration is estimated from the UV-visible spectrophotometer.

$$\text{FAME yield (in mg/L)} = \% \text{ FAME} \times \text{Dry biomass concentration (in mg/L)} \quad (7)$$

3. Results

3.1. Effect of Metal Ions on Methane Oxidation Rates

3.1.1. Copper

With the increase in the copper concentration from 0 to 25 μM , the specific methane oxidation rate increased from 3.25 ± 0.5 to 5.14 ± 0.2 mg CH_4/mg dry biomass/day. Further increase in the copper concentration from 25 to 100 μM did not significantly affect the methane oxidation rate. A high concentration of copper >100 μM decreased the specific methane oxidation rate. With increasing copper concentrations, there was a steady decrease in biomass yield, even at concentrations with enhanced specific methane oxidation rates (Figure 1).

The increasing concentrations of copper led to the loss of sarcina formation (Figure S1 in Supplementary Materials) and induced deformations in the cell morphology, as observed from the SEM micrographs (Figure 2). The accumulation of copper by the organism was confirmed by SEM-EDX analysis of the dried cell mass (Figure 2). The SDS-PAGE analysis of the homogenized biomass grown with various copper concentrations showed an increased intensity of ~45 kDa and ~26 kDa fragments (Figure S2 in Supplementary Mate-

rials), corresponding to the α subunit and β/γ subunits of pMMO, suggesting increased expression of pMMO [27].

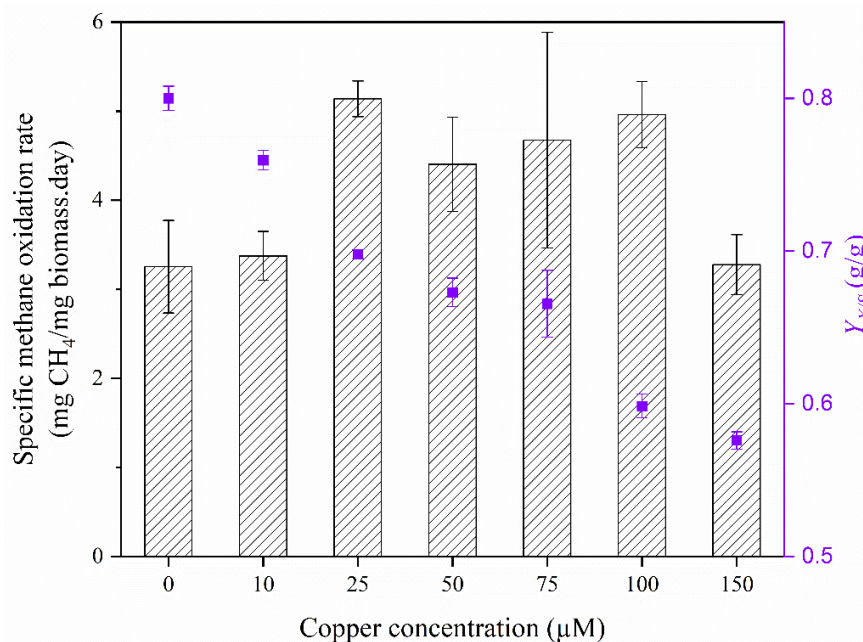


Figure 1. Effect of supplementation by copper on the specific methane oxidation rate and the biomass yield coefficient ($Y_{X/S}$) by *Methylosarcina* sp. LC-4.

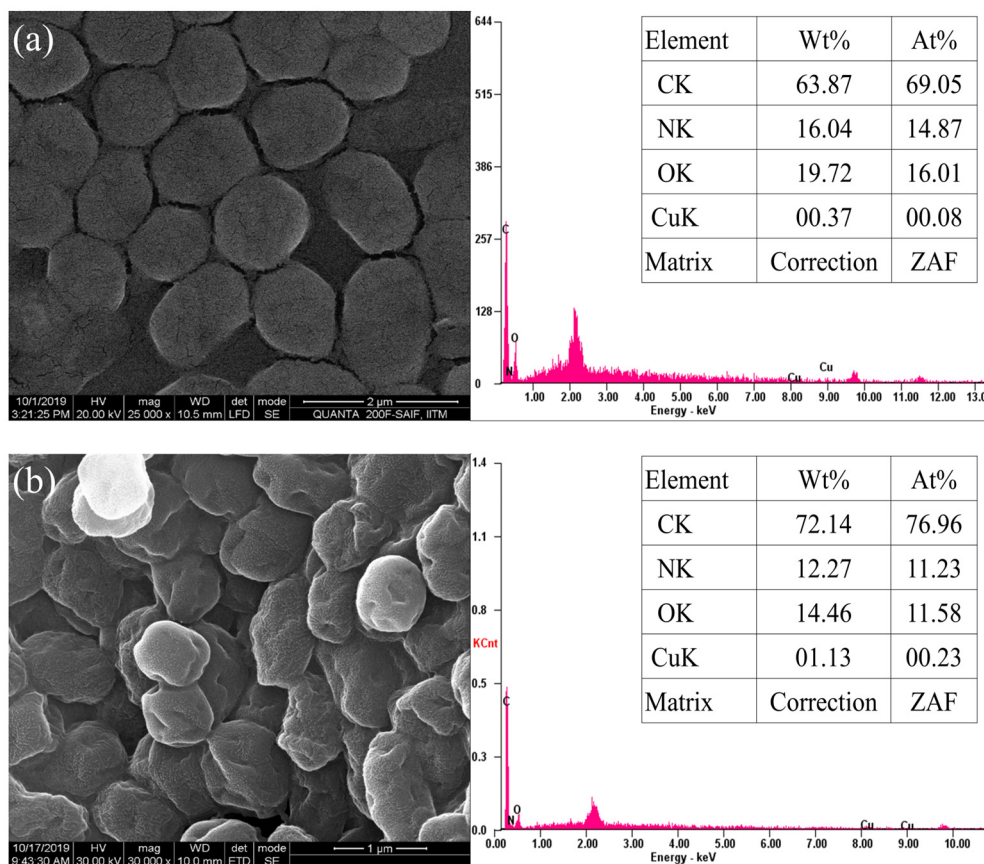


Figure 2. SEM-EDX data taken from biomass grown at different copper concentrations (a) 10 μM and (b) 100 μM .

3.1.2. Cerium

Adding cerium as CeCl_3 to NMS media did not significantly affect the methane oxidation rate or the final biomass concentration of LC-4 when added in the concentration range of 0–10 μM , reportedly inducing the expression of lanthanide-dependent methanol dehydrogenase [28].

3.1.3. Tungstate

The supplementation of NMS media with up to 0.5 μM tungstate led to a more than twofold increase in the specific methane oxidation rate, from 3.37 ± 0.27 to $7.93 \text{ mg CH}_4/\text{mg dry biomass/day}$. Further increased tungstate concentrations were detrimental to methane oxidation rates, and at 1 μM tungstate, the growth of LC-4 was completely inhibited. However, similar to copper supplementation, there was a steady decrease in biomass yield, even at concentrations at enhanced specific methane oxidation rates (Figure 3). The LC-4 cells grown in media supplemented with tungstate showed high nitroblue tetrazolium (NBT) reduction and accumulation in comparison to the cells grown without tungstate, suggesting an increase in the reducing power of the organism; this can be corroborated with the increase in the formate dehydrogenase activity when grown with tungstate [29,30] (Figure S3 in Supplementary Materials).

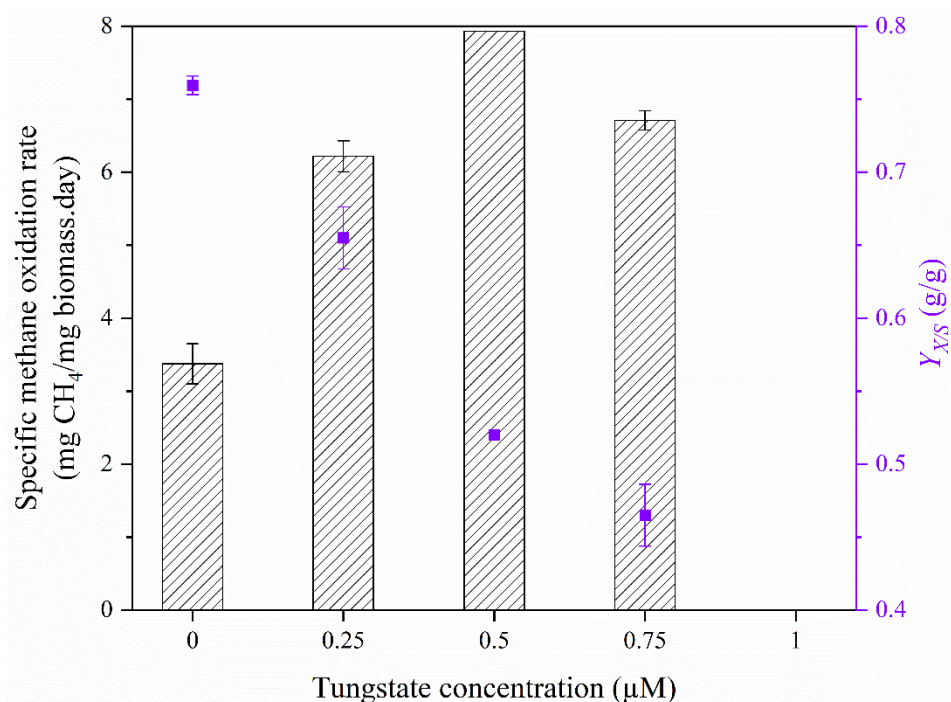


Figure 3. Effect of supplementation by tungstate on the specific methane oxidation rate and the biomass yield coefficient ($Y_{X/S}$) by *Methylosarcina* sp. LC-4.

3.2. Determination of Significant Components in the NMS Media Using the Plackett–Burman Design (PBD)

Seven variables described above were screened with eight experiments in PBD, as summarized in Table 1. The total FAME concentration (mg/L) determined from the biomass concentration (mg/L) and % FAME, as described earlier, was considered the output variable. Values of FAME concentration in all eight experiments conducted according to PBD are specified in Table 2. The biomass yield varied widely from $38.8 \pm 3 \text{ mg/L}$ to $312.7 \pm 11.6 \text{ mg/L}$, with FAME yields ranging from $4.1 \pm 0.3 \text{ mg/L}$ to $48.7 \pm 1.6 \text{ mg/L}$. The contribution of each component considered in PBD and its statistical significance were determined from the ANOVA analysis, as summarized in Table 3. The significant variables were selected based on the p -value, and the variables with a p -value of < 0.05 were considered accurate.

The results suggest that 6 components from the NMS media significantly affected the FAME yield with a p -value < 0.0001 . Cerium showed a very negligible effect, corroborating the obtained batch studies data. A significant inhibitory effect by copper, salinity (NaCl), and magnesium was observed, while nitrogen, tungstate, and phosphate contributed positively (Table 3). A Pareto chart represents the relative significance level of the nutrients on lipid biosynthesis (Figure 4). Based on the p -value of various factors, a first-order polynomial equation was constructed considering the significant factors. ANOVA was used for the statistical analyses of the model. The regression analyses of the model showed a high determination coefficient (R^2) of 0.99, indicating that the model is 99% accurate for the data. The coefficient of variation (CV), F -value, and p -value obtained in this model are 11.38%, 252.5, and < 0.0001 , respectively.

Table 3. Statistical analysis of the NMS media components considered in the Plackett–Burman design.

Symbol	Component	Effect	Contribution (%)	F -Value	p -Value
A	Nitrogen	14.46	7.6	85.44	< 0.0001
B	Phosphorus	6.45	1.5	16.99	0.0008
C	Copper	−30	33.3	367.93	< 0.0001
D	Tungstate	14.25	7.7	83.05	< 0.0001
E	Cerium	0.39	0.005	0.06	0.81
F	Magnesium	−21.99	17.8	197.6	< 0.0001
G	Salinity (NaCl)	−28.80	30.7	339.05	< 0.0001

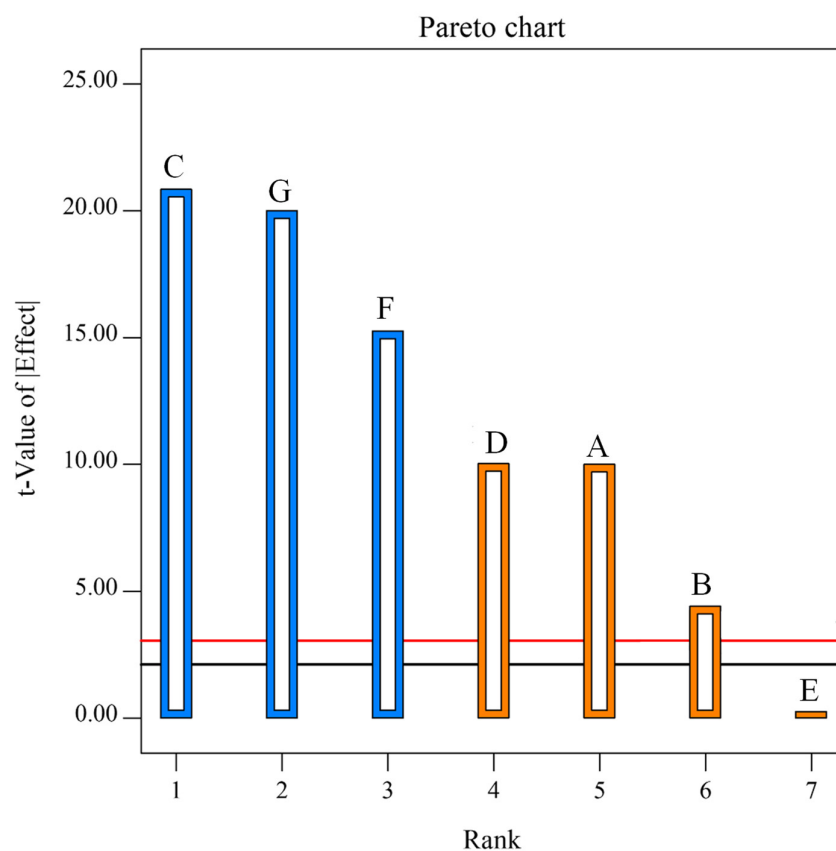


Figure 4. Pareto chart of the Plackett–Burman design representing the effect of various components of the NMS media on the FAME yield. Blue and orange bars indicate negative and positive effects, respectively. The black line refers to the t -value limit, and the red line refers to Bonferroni limit.

3.3. Effect of Optimized Media on FAME Content and Composition

The modified NMS media containing 0.2 g/L of MgSO₄ supplemented with 25 µM of CuSO₄ and 0.5 µM Na₂WO₄, with the remaining components unchanged, was formulated based on the PBD experiment. Using the optimized media improved the FAME yield by almost 85.7%, from 28 ± 0.4 mg/L in unmodified NMS to 52 ± 0.6 mg/L with modified NMS.

This increase was contributed by both an increase in biomass yields and the lipid content of the biomass. The composition of the FAME obtained from the organism LC-4 grown on NMS and modified-NMS media is mentioned in Table 4.

Table 4. Fatty acid composition of lipids from LC-4 grown in NMS and modified NMS media.

FAME (mg/L)	NMS Media	
	28	52
	FAME composition	
C14:0	3.87	7.31
ΣC14:1	5.59	7.78
C15:0	2.76	14.03
ΣC15:1	-	10.78
C16:0	23.49	26.37
ΣC16:1	34.09	17.77
C18:0	5.17	9.63
ΣC18:1	-	6.76
C ₁₄ –C ₁₈	97.58	89.65
C ₁₄ –C ₁₈ unsaturated FAME	50.46	32.31
C ₁₄ –C ₁₈ saturated FAME	47.12	57.34
Total unsaturated FAME	52.1	34.43
Total saturated FAME	47.9	65.61

4. Discussion

Methanotrophs are unique bacteria having the capability to oxidize and assimilate methane. However, the research on methanotrophs is still in its infancy. Optimized media conditions are necessary for improved yields of biomass and derived value-added products from methanotrophs [17]. Although methanotrophic bacteria are subdivided into three types based on the pathway by which they assimilate methane, the central metabolic pathway by which they oxidize methane to carbon dioxide to generate energy is common in all methanotrophs (Figure 5) [21].

The first step in the methane assimilation pathway is the oxidation of methane to methanol by the enzyme methane monooxygenase (MMO), which is restricted only to methanotrophs. MMOs can be of two types: particulate membrane-bound (pMMO) form and soluble form (sMMO) in the cytoplasm [31]. pMMO is the most predominant form of MMO expressed by methanotrophs [32]. pMMO is a metalloenzyme composed of three subunits with copper in its active site. The available copper in the media regulates its activity and expression [31]. In methanotrophs that can express both sMMO and pMMO, the expression of specific MMO is regulated by a copper switch. At high copper, biomass ratio, expression of sMMO is inhibited, and there is an increase in the levels of pMMO [33]. In addition, copper plays a profound role in methane metabolism by inducing the development of internal membranes, leading to increased surface area for housing pMMO and inducing the expression of the downstream formaldehyde dehydrogenases and other proteins involved in copper assimilation, regulation, and transport [27]. Thus, the availability

of copper strongly influences the methane oxidation rate and methanotrophic activity in the environment. *Methylosarcina* sp. LC-4 is a type-I methanotroph and expresses pMMO only [22]. The effect of the available copper concentration on the methane oxidation rate by LC-4 was studied in a shake flask. Furthermore, it was observed that supplementation with 25 μM copper enhanced specific methane oxidation by 58%, which can be attributed to the increase in activity and expression of pMMO from the SDS-PAGE analysis. Higher concentrations of copper ($>50 \mu\text{M}$) are known to inhibit pMMO activity [34]. SEM images of the organism grown at increasing copper concentrations also suggest a change in the morphology of the organism when grown at concentrations of copper with loss of the sarcina-like form, which might be due to its toxic effect.

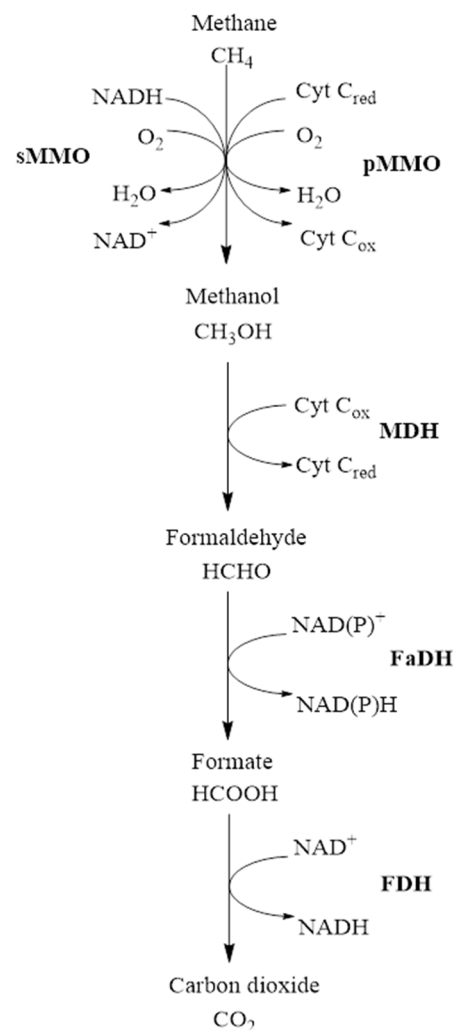


Figure 5. Central metabolic pathway in methanotrophs from oxidation of methane to carbon dioxide (sMMO: soluble methane monooxygenase; pMMO: particulate methane monooxygenase; MDH: methanol dehydrogenase; FaDH: formaldehyde dehydrogenase; FDH: formate dehydrogenase).

Methanol dehydrogenase is a periplasmic membrane-associated protein that is known to function in close association with pMMO. Methanol dehydrogenase oxidizes methanol to formaldehyde with the generation of reduced cofactor shuttled to pMMO [35,36]. Methanol dehydrogenase is also known to occur in two forms: calcium-dependent *MxaB* and lanthanide-dependent *XoxF* [33]. Supplementation of lanthanides, such as cerium (III) and lanthanum (III), in the media is known to induce *XoxF* and suppress the expression of *MxaB* in a few methanotrophs [28]. In the methanotroph, *Methylophilum alcaliphilum* 20Z^R, expression of *XoxF*-methanol dehydrogenase led to increased growth and methane

uptake rates [37]. However, supplementation of cerium as CeCl_3 did not significantly affect the methane oxidation rate or final biomass concentration in LC-4.

The oxidation of formate catalyzed by formate dehydrogenases is the last step in the oxidation of methane to carbon dioxide. Formate dehydrogenases are also metalloenzymes requiring either tungstate or molybdate for activity [38]. When LC-4 was grown on methane, it was observed that organic acid, predominantly formate, was released into the medium. This formate was later slowly oxidized to carbon dioxide [22]. This suggested that formate oxidation by formate dehydrogenase might be the rate-limiting step. Since the NMS media already contained molybdate, the effect of tungstate supplementation on methane oxidation was studied. Adding up to $0.5 \mu\text{M}$ tungstate led to a more than twofold increase in the specific methane oxidation rate. This step generates a reducing equivalent of NAD(P)H, which might provide electrons for methane oxidation by pMMO. Increased formate dehydrogenase activity in biomass grown in tungstate-supplemented media corroborates that the increased methane oxidation rate is attributed to reduced cofactor availability. These results are consistent with the experimental studies and the literature, where external formate supplementation leads to increased conversion of methane to methanol [39].

Despite the increase in the methane uptake rate with the addition of copper and tungstate, the biomass yields decreased. It was suspected that growth in a shake flask led to severe gas–liquid mass transfer limitations for methane. Since the equation relates maximum biomass concentrations and methane transport rate, the increase in specific methane oxidation/consumption rates (q_{methane}) leads to lower maximum biomass concentrations due to limited gas–liquid mass transfer for methane (Equation (8)) [40].

$$X_{\text{max}} = \frac{k_L a C^*}{q_{\text{methane}}} \quad (8)$$

where X_{max} is the maximum biomass concentration, $k_L a$ is the mass transfer coefficient of methane, and C^* is the saturating concentration of methane in the liquid phase.

The typical values for $k_L a$ for shake-flask cultivation range from $25\text{--}50 \text{ h}^{-1}$ for oxygen, and methane values are typically 85% of the value for oxygen [40]. Thus, a $k_L a$ of 30 h^{-1} and headspace methane concentration of 3% limits biomass concentrations to 135 mg/L for q_{methane} of $3.37 \text{ mg CH}_4/\text{mg dry biomass/day}$ and to only 60 mg/l for q_{methane} of $7.93 \text{ mg CH}_4/\text{mg dry biomass/day}$. Thus, meaningful interpretation of results on enhanced methane oxidation needs experimental setups that support better gas–liquid mass transfer. Hence, further experiments were carried out in stirred reactor bottles, allowing for better $k_L a$ owing to better mixing efficiency at higher mixing speed [41]. Additionally, the culture volumes were scaled up to 600 mL to allow biodiesel extraction from the cultured conditions.

A Plackett–Burman Design (PBD) is a widely used statistical method for screening and preliminary optimization of important components in culture media. In the present study, PBD was adopted to find the most significant components among the macro and micronutrients in the NMS media contributing to both the biomass and lipid synthesis analyzed in the form of fatty acid methyl esters (FAME), as described in Section 2.5 of this study. In addition to the micronutrients copper, cerium, and tungstate that play a pivotal role in the central metabolic pathway, magnesium (as MgSO_4), phosphorus (as phosphate), and nitrogen (as nitrate) were considered variables in the PBD. In addition to being important macronutrients essential for growth, they also influence lipid accumulation in several ways. Magnesium is an essential cofactor for pyruvate dehydrogenase, the key enzyme that controls the carbon flux [42]. It is also known to inhibit methanol dehydrogenase activity in methanotrophs [43]. Phosphorus and nitrogen are essential components of biomass, and their limitation leads to a slowdown of cell proliferation and promotes lipid accumulation in many organisms [44,45]. In a recent report, phosphate limitation leads to remodeling the membrane lipids in the methanotroph *Methylosinus trichosporium* OB3b [46]. Salinity-induced stress also leads to lipid remodeling with more acid phospholipids and

unbranched fatty acids in *Methylobacterium alcaliphilus* 20Z [47]. Hence, sodium chloride (NaCl) was also considered a parameter in the PBD.

Copper showed the most significant adverse effect on biomass and FAME yields. As discussed previously, beyond specific concentrations, copper exerts a toxic effect on most organisms, as is evident in the scanning electron micrographs of LC-4. Salinity and magnesium also displayed a strong negative effect on biomass yields. The negative impact of magnesium and sodium chloride is likely due to the inhibitory effect on the calcium-dependent methanol dehydrogenase, one of the central enzymes in methane metabolism, which catalyzes the conversion of methanol to formate [48]. Inhibition by magnesium and no significant effect due to cerium indicate the absence of lanthanide-dependent methanol dehydrogenase in LC-4. The inhibition of methanol dehydrogenase decreases the carbon flux to the RuMP pathway for biomass formation, thus, contributing to the overall decrease in the biomass and the total lipid. Although the negative impact on the biomass and FAME concentration was more evident in comparison to the positive effect in the experimental design, the positive influence of nitrogen, tungstate, and phosphate in total, contributing 16.8%, cannot be neglected (Table 3). Nitrogen and phosphorus are essential components of biomass and are expected to benefit biomass yields. In type-I methanotrophs expressing pMMO, membrane lipids containing phospholipids constitute the major fraction of the total lipids; these membrane lipids act as a housing for pMMO, a membrane protein that alone contributes to 20% of the total protein. Limitations in either nitrogen or phosphorus, thus, directly influence the growth and biomass yield, affecting the overall FAME yields. In addition, tungstate contributed 7.7% to the FAME yields, among the various factors considered. As discussed earlier, tungstate, the cofactor for formate dehydrogenase, is expected to improve the methane uptake rate and biomass yields by providing the extra reducing equivalents obtained from formate oxidation to the pMMO enzyme.

The modified NMS media formulated based on the PBD resulted in about 86% of the FAME yield. The FAME content of $13 \pm 1\%$ is among the highest in methanotrophs, others being 9.5–10.7% in *Methylobacterium buryatense* 5GB1, 9% in *Methylocystis* sp. Rockwell, and 13% in *Methylobacterium methanica* [19,20,49,50]. The FAME composition also changed compared to FAME from the organism LC-4 grown on unmodified NMS media. The physical and chemical properties of biodiesel are dependent on its FAME composition. Fatty acids belonging to C₁₄–C₁₈ are considered the most suitable for biodiesel applications. In the present study, the significant fraction of FAME in the modified NMS media is palmitic acid (C16:0) and Σ C16:1, with 26.37% and 17.77%, respectively, the characteristic feature of type-I methanotrophs. The other major fatty acids include pentadecanoic acid (C15:0), Σ C15:1, stearic acid (C18:0), and Σ C18:1. Although there was a decrease in the C₁₄–C₁₈ FAME fraction from 97.6% to 89.7%, the saturated fraction increased from 47% to 57% when LC-4 was grown in the optimized media. The ratio of saturated to unsaturated fatty acids is an important factor in choosing biodiesel for usage. Saturated fatty acids contribute to a higher cetane number and stability from oxidative damage, whereas unsaturated fatty acids prevent solidification in low temperatures. The saturated to unsaturated fatty acids (C₁₄–C₁₈) are higher in FAME from modified NMS media (57.3:32.3) in comparison to NMS media (47.1:50.5).

Thus, media optimization using the Plackett–Burman design led to improved yields of FAME and a higher fraction of saturated fatty acids, improving the applicability for use as biodiesel. Further, scale-up studies involving continuous cultivation in a reactor can lead to the increased productivity of biomass and, in turn, lipids, making the biological gas-to-liquid technology for converting methane to liquid biofuels a practical and viable process for conversion of both the concerns of greenhouse gas emissions and sustainable biofuel production.

5. Summary and Conclusions

Methylosarcina sp. LC-4 is a pMMO-expressing type-I and a model methanotroph that has the potential for applications in bio-augmented systems in mitigating low concentrations of methane. The specific methane uptake rate and the methane capture in biomass are greatly influenced by the chemical composition of media, especially the micronutrients that act as cofactors for vital enzymes involved in the metabolic pathway of methane assimilation. In the present study, the specific methane uptake rate by the isolate LC-4 was improved from 3.25 ± 0.5 to 5.14 ± 0.2 mg CH₄/mg dry biomass/day and from 3.37 ± 0.27 to 7.93 mg CH₄/mg dry biomass/day by the supplementation of copper and tungstate, respectively, thus, making it a robust organism for biological methane fixation and other industrial applications. The effect of micro and macronutrients present in the NMS media on the biomass and fatty acid methyl ester (FAME) yield of LC-4 was studied in a pragmatic approach using the Plackett–Burman design, and the critical nutrients were optimized. As a result, the FAME yield increased from 28 ± 0.4 mg/L in unmodified NMS to 52 ± 0.6 mg/L with a FAME content of $13 \pm 1\%$, the highest among the methanotrophs reported to date. Upon analyzing the FAME content, 89.6% of the fatty acids belong to the C₁₄–C₁₈ fraction, with palmitic acid (C16:0) and Σ C16:1 as the major fraction, making it suitable for use as biodiesel. Considering the need to curb methane emissions and to generate clean, renewable energy, the productivity using *Methylosarcina* sp. LC-4 can further be improved by increasing the solubility of methane.

Supplementary Materials: The following supporting information can be downloaded at: <https://www.mdpi.com/article/10.3390/su15010505/s1>. Figures S1–S3 are available in the supplementary data provided.

Author Contributions: N.S.: Conceptualization, methodology, formal analysis, investigation, data curation, writing—original draft preparation; D.N.A. and C.K.: Conceptualization, validation, resources, writing—review and editing, visualization, supervision, D.N.A.: Project administration. All authors have read and agreed to the published version of the manuscript.

Funding: This research received no external funding.

Institutional Review Board Statement: Not applicable.

Informed Consent Statement: Not applicable.

Data Availability Statement: All data used during the study appear in the submitted article. There are no codes and models associated with this submission.

Acknowledgments: One of the authors, Nivedita Sana, expresses her gratitude to IIT Madras, India, for the fellowship. Also, the authors acknowledge the Sophisticated Analytical Instrument Facility (SAIF), IIT Madras, for the SEM-EDX analysis.

Conflicts of Interest: The authors declare no conflict of interest.

References

1. Keasling, J.; Garcia Martin, H.; Lee, T.S.; Mukhopadhyay, A.; Singer, S.W.; Sundstrom, E. Microbial Production of Advanced Biofuels. *Nat. Rev. Microbiol.* **2021**, *19*, 701–715. [[CrossRef](#)] [[PubMed](#)]
2. Ahmad, F.B.; Zhang, Z.; Doherty, W.O.S.; O'Hara, I.M. A Multi-Criteria Analysis Approach for Ranking and Selection of Microorganisms for the Production of Oils for Biodiesel Production. *Bioresour. Technol.* **2015**, *190*, 264–273. [[CrossRef](#)] [[PubMed](#)]
3. Blanch, H.W.; Simmons, B.A.; Klein-Marcuschamer, D. Biomass Deconstruction to Sugars. *Biotechnol. J.* **2011**, *6*, 1086–1102. [[CrossRef](#)] [[PubMed](#)]
4. Zhang, L.; Loh, K.C.; Kuroki, A.; Dai, Y.; Tong, Y.W. Microbial Biodiesel Production from Industrial Organic Wastes by Oleaginous Microorganisms: Current Status and Prospects. *J. Hazard. Mater.* **2021**, *402*, 123543. [[CrossRef](#)] [[PubMed](#)]
5. Fei, Q.; Guarnieri, M.T.; Tao, L.; Laurens, L.M.L.; Dowe, N.; Pienkos, P.T. Bioconversion of Natural Gas to Liquid Fuel: Opportunities and Challenges. *Biotechnol. Adv.* **2014**, *32*, 596–614. [[CrossRef](#)] [[PubMed](#)]
6. Zhang, C.; Ottenheim, C.; Weingarten, M.; Ji, L.H. Microbial Utilization of Next-Generation Feedstocks for the Biomanufacturing of Value-Added Chemicals and Food Ingredients. *Front. Bioeng. Biotechnol.* **2022**, *10*, 874612. [[CrossRef](#)] [[PubMed](#)]
7. Holmes, D.E.; Smith, J.A. Biologically Produced Methane as a Renewable Energy Source. *Adv. Appl. Microbiol.* **2016**, *97*, 1–61. [[CrossRef](#)]

8. Comer, A.D.; Long, M.R.; Reed, J.L.; Pfleger, B.F. Flux Balance Analysis Indicates That Methane Is the Lowest Cost Feedstock for Microbial Cell Factories. *Metab. Eng. Commun.* **2017**, *5*, 26–33. [[CrossRef](#)]
9. McArthur, J.-A. Methane Emissions Are Driving Climate Change. Here's How to Reduce Them. Available online: <https://www.unep.org/news-and-stories/story/methane-emissions-are-driving-climate-change-heres-how-reduce-them> (accessed on 15 July 2022).
10. Haynes, C.A.; Gonzalez, R. Rethinking Biological Activation of Methane and Conversion to Liquid Fuels. *Nat. Chem. Biol.* **2014**, *10*, 331–339. [[CrossRef](#)]
11. Karakurt, I.; Aydin, G.; Aydiner, K. Sources and Mitigation of Methane Emissions by Sectors: A Critical Review. *Renew. Energy* **2012**, *39*, 40–48. [[CrossRef](#)]
12. Gebauer, J.P.; Kaltschmitt, M. Bio-Gtl Processes. In *Energy from Organic Materials (Biomass)*; Springer: New York, NY, USA, 2019; pp. 1145–1174.
13. Zappi, A.; Fortela, D.L.; Holmes, W.E. An Assessment of Methanotrophs Producing Industrial-Grade Lipids for Biofuels and Other Commercial Chemicals. *Energies* **2020**, *13*, 3887. [[CrossRef](#)]
14. Guerrero-Cruz, S.; Vaksmaa, A.; Horn, M.A.; Niemann, H.; Pijuan, M.; Ho, A. Methanotrophs: Discoveries, Environmental Relevance, and a Perspective on Current and Future Applications. *Front. Microbiol.* **2021**, *12*, 678057. [[CrossRef](#)] [[PubMed](#)]
15. Kim, I.T.; Ahn, K.H.; Lee, Y.E.; Jeong, Y.; Park, J.R.; Shin, D.C.; Jung, J. An Experimental Study on the Biological Fixation and Effective Use of Carbon Using Biogas and Bacterial Community Dominated by Methanotrophs, Methanol-Oxidizing Bacteria, and Ammonia-Oxidizing Bacteria. *Catalysts* **2021**, *11*, 1342. [[CrossRef](#)]
16. Strong, P.J.; Xie, S.; Clarke, W.P. Methane as a Resource: Can the Methanotrophs Add Value? *Environ. Sci. Technol.* **2015**, *49*, 4001–4018. [[CrossRef](#)] [[PubMed](#)]
17. Gesicka, A.; Oleskiewicz-Popiel, P.; Łężyk, M. Recent Trends in Methane to Bioproduct Conversion by Methanotrophs. *Biotechnol. Adv.* **2021**, *53*, 107861. [[CrossRef](#)]
18. Kalyuzhnaya, M.G. Methane Biocatalysis: Selecting the Right Microbe. In *Biotechnology for Biofuel Production and Optimization*; Elsevier: Amsterdam, The Netherlands, 2016; pp. 353–383. ISBN 9780444634757.
19. Gilman, A.; Laurens, L.M.; Puri, A.W.; Chu, F.; Pienkos, P.T.; Lidstrom, M.E. Bioreactor Performance Parameters for an Industrially-Promising Methanotroph *Methylobacterium Buryatense* 5GB1. *Microb. Cell Factories* **2015**, *14*, 182. [[CrossRef](#)]
20. Dong, T.; Fei, Q.; Genelot, M.; Smith, H.; Laurens, L.M.L.; Watson, M.J.; Pienkos, P.T. A Novel Integrated Biorefinery Process for Diesel Fuel Blendstock Production Using Lipids from the Methanotroph, *Methylobacterium Buryatense*. *Energy Convers. Manag.* **2017**, *140*, 62–70. [[CrossRef](#)]
21. Hanson, R.S.; Hanson, T.E. Methanotrophic Bacteria. *Microbiol. Rev.* **1996**, *60*, 439–471. [[CrossRef](#)]
22. Nivedita, S.; Arnepalli, D.N.; Krishnan, C. Kinetics and Stoichiometry of an Efficient Methanotroph *Methylosarcina* Sp. LC-4 Isolated from a Municipal Solid Waste Dumpsite. *J. Environ. Eng.* **2021**, *147*, 04021011. [[CrossRef](#)]
23. Whiddon, K.T.; Gudneppanavar, R.; Hammer, T.J.; West, D.A.; Konopka, M.C. Fluorescence-based Analysis of the Intracytoplasmic Membranes of Type I Methanotrophs. *Microb. Biotechnol.* **2019**, *12*, 1024–1033. [[CrossRef](#)]
24. D'Ambrosio, V.; Scelsi, E.; Pastore, C. Non-Edible Oils for Biodiesel Production. In *Biodiesel Production*; John Wiley & Sons, Ltd.: New Jersey, NJ, USA, 2022; pp. 49–66.
25. Chamola, R.; Khan, M.F.; Raj, A.; Verma, M.; Jain, S. Response Surface Methodology Based Optimization of in Situ Transesterification of Dry Algae with Methanol, H₂SO₄ and NaOH. *Fuel* **2019**, *239*, 511–520. [[CrossRef](#)]
26. Pereira, E.; Napp, A.; Braun, J.V.; Fontoura, L.A.M.; Seferin, M.; Ayres, J.; Ligabue, R.; Passaglia, L.M.P.; Vainstein, M.H. Development and Validation of Analytical Methodology by GC-FID Using Hexadecyl Propanoate as an Internal Standard to Determine the Bovine Tallow Methyl Esters Content. *J. Chromatogr. B* **2018**, *1093–1094*, 134–140. [[CrossRef](#)] [[PubMed](#)]
27. Semrau, J.D.; DiSpirito, A.A.; Yoon, S. Methanotrophs and Copper. *FEMS Microbiol. Rev.* **2010**, *34*, 496–531. [[CrossRef](#)]
28. Picone, N.; Op den Camp, H.J. Role of Rare Earth Elements in Methanol Oxidation. *Curr. Opin. Chem. Biol.* **2019**, *49*, 39–44. [[CrossRef](#)] [[PubMed](#)]
29. Urban, T.; Jarstrand, C. Nitroblue Tetrazolium (NBT) Reduction by Bacteria. *Acta Pathol. Microbiol. Scand. Sect. B Microbiol.* **2009**, *87B*, 227–233. [[CrossRef](#)]
30. Wang, H.; Wang, F.; Tao, X.; Cheng, H. Ammonia-containing dimethyl sulfoxide: An improved solvent for the dissolution of formazan crystals in the 3-(4,5-dimethylthiazol-2-yl)-2,5-diphenyl tetrazolium bromide (MTT) assay. *Anal. Biochem.* **2012**, *421*, 324–326. [[CrossRef](#)]
31. Ross, M.O.; Rosenzweig, A.C. A Tale of Two Methane Monooxygenases. *J. Biol. Inorg. Chem.* **2017**, *22*, 307–319. [[CrossRef](#)]
32. Semrau, J.D.; DiSpirito, A.A.; Vuilleumier, S. Facultative Methanotrophy: False Leads, True Results, and Suggestions for Future Research. *FEMS Microbiol. Lett.* **2011**, *323*, 1–12. [[CrossRef](#)]
33. Semrau, J.D.; DiSpirito, A.A.; Gu, W.; Yoon, S. Metals and Methanotrophy. *Appl. Environ. Microbiol.* **2018**, *84*, e02289-17. [[CrossRef](#)]
34. Chidambarampadmavathy, K.; Obulisamy, P.K.; Heimann, K. Role of Copper and Iron in Methane Oxidation and Bacterial Biopolymer Accumulation. *Eng. Life Sci.* **2015**, *15*, 387–399. [[CrossRef](#)]
35. Culpepper, M.A.; Rosenzweig, A.C. Structure and Protein-Protein Interactions of Methanol Dehydrogenase from *Methylococcus Capsulatus* (Bath). *Biochemistry* **2014**, *53*, 6211–6219. [[CrossRef](#)] [[PubMed](#)]
36. Deng, Y.W.; Ro, S.Y.; Rosenzweig, A.C. Structure and Function of the Lanthanide-Dependent Methanol Dehydrogenase XoxF from the Methanotroph *Methylobacterium Buryatense* 5GB1C. *J. Biol. Inorg. Chem.* **2018**, *23*, 1037–1047. [[CrossRef](#)] [[PubMed](#)]

37. Akberdin, I.R.; Collins, D.A.; Hamilton, R.; Oshchepkov, D.Y.; Shukla, A.K.; Nicora, C.D.; Nakayasu, E.S.; Adkins, J.N.; Kalyuzhnaya, M.G. Rare Earth Elements Alter Redox Balance in Methylobacterium Alcaliphilum 20ZR. *Front. Microbiol.* **2018**, *9*, 1–12. [[CrossRef](#)] [[PubMed](#)]
38. Hartmann, T.; Schwanhold, N.; Leimkühler, S. Assembly and Catalysis of Molybdenum or Tungsten-Containing Formate Dehydrogenases from Bacteria. *Biochim. Et Biophys. Acta Proteins Proteom.* **2015**, *1854*, 1090–1100. [[CrossRef](#)] [[PubMed](#)]
39. Bak, S.Y.; Kang, S.G.; Choi, K.H.; Park, Y.R.; Lee, E.Y.; Park, B.J. Phase-Transfer Biocatalytic Methane-to-Methanol Conversion Using the Spontaneous Phase-Separable Membrane MCSTR. *J. Ind. Eng. Chem.* **2022**, *111*, 389–397. [[CrossRef](#)]
40. Meraz, J.L.; Dubrawski, K.L.; Abbadi, S.H.E.; Choo, K.-H.; Criddle, C.S. Membrane and Fluid Contactors for Safe and Efficient Methane Delivery in Methanotrophic Bioreactors. *J. Environ. Eng.* **2020**, *146*, 03120006. [[CrossRef](#)]
41. Klöckner, W.; Gacem, R.; Anderlei, T.; Raven, N.; Schillberg, S.; Lattermann, C.; Büchs, J. Correlation between Mass Transfer Coefficient K_La and Relevant Operating Parameters in Cylindrical Disposable Shaken Bioreactors on a Bench-to-Pilot Scale. *J. Biol. Eng.* **2013**, *7*, 1–14. [[CrossRef](#)]
42. Midgley, J.W.; Rutter, G.A.; Thomas, A.P.; Denton, R.M. Effects of Ca^{2+} and Mg^{2+} on the Activity of Pyruvate Dehydrogenase Phosphate Phosphatase within Toluene-Permeabilized Mitochondria. *Biochem. J.* **1987**, *241*, 371–377. [[CrossRef](#)]
43. Patel, S.K.S.; Shanmugam, R.; Kalia, V.C.; Lee, J.K. Methanol Production by Polymer-Encapsulated Methanotrophs from Simulated Biogas in the Presence of Methane Vector. *Bioresour. Technol.* **2020**, *304*, 123022. [[CrossRef](#)]
44. Anto, S.; Pugazhendhi, A.; Mathimani, T. Lipid Enhancement through Nutrient Starvation in *Chlorella* Sp. and Its Fatty Acid Profiling for Appropriate Bioenergy Feedstock. *Biocatal. Agric. Biotechnol.* **2019**, *20*, 101179. [[CrossRef](#)]
45. Kumar, R.; Dhanarajan, G.; Sarkar, D.; Sen, R. Multi-Fold Enhancement in Sustainable Production of Biomass, Lipids and Biodiesel from Oleaginous Yeast: An Artificial Neural Network-Genetic Algorithm Approach. *Sustain. Energy Fuels* **2020**, *4*, 6075–6084. [[CrossRef](#)]
46. Scanlan, J.; Guillonneau, R.; Cunningham, M.R.; Najmin, S.; Matusz, M.A.; Murphy, A.; Murray, L.L.; Zhang, L.; Kumaresan, D.; Chen, Y. The Proteobacterial Methanotroph Methylosinus Trichosporium OB3b Remodels Membrane Lipids in Response to Phosphate Limitation. *Front. Microbiol.* **2022**, *13*, 1–14. [[CrossRef](#)] [[PubMed](#)]
47. Strong, P.J.; Kalyuzhnaya, M.; Silverman, J.; Clarke, W.P. A Methanotroph-Based Biorefinery: Potential Scenarios for Generating Multiple Products from a Single Fermentation. *Bioresour. Technol.* **2016**, *215*, 314–323. [[CrossRef](#)] [[PubMed](#)]
48. AlSayed, A.; Fergala, A.; Khattab, S.; ElSharkawy, A.; Eldyasti, A. Optimization of Methane Bio-Hydroxylation Using Waste Activated Sludge Mixed Culture of Type I Methanotrophs as Biocatalyst. *Appl. Energy* **2018**, *211*, 755–763. [[CrossRef](#)]
49. Burdette, M.D. Production of Biodiesel-like Components by the Type I Methanotroph Methylobacterium Methanica. Master's Thesis, Clemson University, South Carolina, SC, USA, August 2013.
50. Tays, C.; Guarneri, M.T.; Sauvageau, D.; Stein, L.Y. Combined Effects of Carbon and Nitrogen Source to Optimize Growth of Proteobacterial Methanotrophs. *Front. Microbiol.* **2018**, *9*, 2239. [[CrossRef](#)] [[PubMed](#)]

Disclaimer/Publisher's Note: The statements, opinions and data contained in all publications are solely those of the individual author(s) and contributor(s) and not of MDPI and/or the editor(s). MDPI and/or the editor(s) disclaim responsibility for any injury to people or property resulting from any ideas, methods, instructions or products referred to in the content.